Journal of Inflammation Research

Dovepress
open access to scientific and medical research

Open Access Full Text Article

ORIGINAL RESEARCH

The Nrf2 Pathway Alleviates Overloading Force-Induced TMJ Degeneration by Downregulating Oxidative Stress Reactions

Minglu Xu[1,2,*], Lingli Fang[1,2,*], Qin Xue[1,2], Xuyang Zhang[1,2], Yao He[1,3]

[1]Department of Orthodontics, Stomatological Hospital of Chongqing Medical University, Chongqing, People's Republic of China; [2]Chongqing Key Laboratory of Oral Disease and Biomedical Sciences, Stomatological Hospital of Chongqing Medical University, Chongqing, People's Republic of China; [3]Chongqing Municipal Key Laboratory of Oral Biomedical Engineering of Higher Education, Stomatological Hospital of Chongqing Medical University, Chongqing, People's Republic of China

*These authors contributed equally to this work

Correspondence: Yao He, Department of Orthodontics, Stomatological Hospital of Chongqing Medical University, 426 North of Songshi Avenue, Chongqing, 401147, People's Republic of China, Email yaohe@hospital.cqmu.edu.cn

Objective: Oxidative stress is involved in the mechanisms associated with temporomandibular joint (TMJ) diseases. Nuclear factor erythroid 2-related factor 2 (Nrf2) is a crucial oxidative stress marker, but the specific mechanisms of its regulation in the early stages of mandibular condylar cartilage (MCC) degeneration remain unclear. This study aimed to explore the regulatory role of Nrf2 and its related oxidative stress signaling pathway in the early stage of MCC degeneration.

Materials and Methods: Overloading force-induced MCC degeneration was performed in wild-type and Nrf2 knockout mice, as well as in mice after treatment with the Nrf2 activator cardamonin. Changes in MCC degeneration and the expression of oxidative stress markers in the corresponding situations were observed.

Results: Nrf2 and NADPH oxidase 2 (NOX2) expression were elevated during early MCC degeneration induced by an overloading force. MCC degeneration was aggravated when Nrf2 was knocked out, accompanied by increased NOX2 and superoxide dismutase 2 (SOD2) expression. The MCC degeneration process was alleviated after cardamonin treatment, with activation of the Nrf2 pathway and decreased NOX2 and SOD2 expression.

Conclusion: Early MCC degeneration is accompanied by mild oxidative stress progression. Activated Nrf2 and related pathways could alleviate the degeneration of MCC.

Keywords: NF-E2-related factor 2, oxidative stress, temporomandibular joint, cartilage, mechanical force

Introduction

Temporomandibular joint (TMJ) diseases, as the fourth most common disease in dentistry, have a prevalence of 31.1% in adults.[1] Their etiologies are diverse and include age, trauma, malocclusion, induction of rheumatological or systemic inflammatory, posture and certain psychosocial or neurogenic factors.[2–8] Temporomandibular joint diseases can be classified into two categories: those resulting from structural changes and positional changes. Due to altering the loading way of the joint, the structural changes cause pathological changes including inflammation, degeneration and deformation of the mandibular condylar cartilage (MCC).[9] Among them, temporomandibular joint osteoarthritis is an important degenerative disease.[10] Degeneration is mainly manifested by apoptosis of chondrocytes, degradation of the cartilage matrix, and even destruction of cartilage structure, superficial fissures or defects in severe cases. These pathological changes will cause joint dysfunction, such as popping and strangulation of the joint and limitation of mouth opening, which may be accompanied by painful spasms, local swelling and other inflammation.[10] Once the patient progresses to osteoarthritis, normal structure and function are lost, resulting in significant pain and functional impairment.[11] Therefore,

Received: 12 September 2023
Accepted: 10 November 2023
Published: 27 November 2023

appropriate interventions made in the early stages would have a positive effect on the disease prognosis and patient discomfort.

Overloading of the TMJ induces joint degeneration, as evidenced by the reduced thickness of condylar cartilage, disorganized chondrocyte arrangement, reduced extracellular matrix and even the development of osteoarthritis with nesting chondrocyte proliferation.[12,13] Fang et al found that an overloading force imposed for 5 and 10 days induced initial and transitional degeneration in the middle segment of the TMJ cartilage, respectively.[14] This progression was similar to the early stage of joint degeneration in the natural course of the disease.

Regarding the mechanisms of joint degeneration, some studies have focused on oxidative stress. Oxidative stress causes the release of reactive oxygen species (ROS), which can directly or indirectly damage the physiological functions of macromolecules such as proteins, lipids, and nucleic acids in cells.[15,16] Kawai's study first demonstrated ROS in the synovial fluid from TMJ arthritis using an electron spin resonance (ESR) technique.[17] Furthermore, some studies have shown that extra loading, trauma, and degeneration of the TMJ can lead to the release of ROS, causing the onset of oxidative stress and changes in related biomarkers, resulting in painful reactions associated with TMJ diseases.[18–22]

Nuclear factor erythroid 2-related factor 2 (Nrf2), a major transcriptional regulator in the antioxidant system, enters the nucleus in response to oxidative stress after dissociating from Keap1 and subsequently initiates the transcription of various downstream antioxidant factors to exert antioxidant effects.[23] Presently, some studies have reported that Nrf2 may play an anti-inflammatory role in osteoarthritis,[24] while the specific mechanism of Nrf2 in the early pathology of MCC degeneration has not been studied. Cardamonin, a natural plant extract, has shown anti-inflammatory and antioxidant properties to treat and prevent osteoarthritis associated with inflammation and oxidative stress by activating the Nrf2 pathway.[24,25]

To clarify the role of Nrf2 in the early stage of MCC degeneration, an overloading force was imposed on wild-type and Nrf2 knockout (Nrf2-/-) mice. The Nrf2 activator cardamonin was used to affect the early stage of MCC degeneration by regulating the oxidative stress reaction. We observed MCC degeneration, the release of ROS and the expression of oxidative stress-related markers under different conditions. Our study may provide appropriate strategies for the clinical prevention and treatment of TMJ diseases in early stages.

Materials and Methods

These experiments were conducted in accordance with the ethical protocol approved by the Animal Ethics Committee of Chongqing Medical University (AECCMU-2020-004), and all experiments followed the National Institutes of Health's Guidelines for the Care and Use of Laboratory Animals.

Animals

C57BL/6 wild-type male mice were purchased from the Animal Center of Chongqing Medical University, and C57BL/6 Nrf2-/- mice were presented by Prof. Gangyi Yang of the Second Hospital of Chongqing Medical University. All animals were housed at the Experimental Animal Center of Chongqing Medical University Stomatology Hospital, with freely available food and water, maintained at a temperature of 25°C, 40% humidity, and a 12-hour light/dark cycle. Based on the study of Fang et al, eight-week-old mice were immobilized after induction of isoflurane anesthesia 3.0% in 30% oxygen and 70% nitrous oxide, placed in a forced mouth opening device (0.016-inch Australian wire, Special Plus+, A.J. Wilcock), with 0.5 N applied to the TMJ for 1 h/day. Our experiment was divided into three parts as follows. In the first part, force was performed only on wild-type mice, they were divided into a control (con) group, a 5-day (5 d) group with 5 consecutive days of force imposing, and a 10-day (10 d) group with 10 consecutive days of force imposing (n = 6 per group). In the second part, force was performed on Nrf2-/- mice. Nrf2-/- mice were used as the experimental group and Nrf2+/+ from the same litter as the control group, and overloading force was applied for 5 and 10 consecutive days, respectively. They were divided into the following four groups: Nrf2-5d-con (N-5C), Nrf2-5d-ex (N-5E), Nrf2-10d-con (N-10C) and Nrf2-10d-ex (N-10E) groups (n = 5 per group). In the third part, overloading force was applied in wild-type mice after intraperitoneal injection of cardamonin (M5301, AbMole, USA) for 5 and 10 consecutive days, respectively. Cardamonin was injected two days before force overloading at a dose of 50 mg/kg daily until the end of the experiment, while control mice were injected with blank drug in the same way. These mice were divided into Cardamonin-5d-con

(C-5C), Cardamonin-5d-ex (C-5E), Cardamonin −10d-con (C-10C) and Cardamonin-10d-ex (C-10E) groups (n = 6 per group). Finally, all mice were euthanized in a carbon dioxide (CO_2)-filled euthanasia chamber.

Genotyping

Mouse toe was taken and immersed in lysis solution (AG12307, Accurate Biotechnology, Hunan, China) configured according to the instructions and heated in a water bath at 65°C for 2 hours, followed by heating at 98°C for one minute. After cooling to room temperature and centrifugation at 12,000 rpm for 10 minutes at 4°C, supernatant was taken for polymerase chain reaction (PCR) amplification. The primers used in the PCR assay are shown in Table 1. The PCR product was analyzed on a 3% TAE agarose gel, confirmed Nrf2-/- and Nrf2+/+ genotype at 400 bp and 262 bp sizes, respectively (Figure S1A, B).

Specimen Processing

After execution of the mice, the head was incised sagittally. The intact right condyle was isolated, and the disc was stripped. Condyle was used for confocal, microcomputed tomography (Micro-CT) analysis, and scanning electron microscopy (SEM). Discs were immersed in optimum cutting temperature compound (O.C.T. Compound, Solarbio, China) for frozen sections. The left side of the head was immersed in 10% paraformaldehyde (PFA, Affymetrix, Cleveland, OH) and fixed at 4°C for 24 hours, decalcified with 19% ethylene diamine tetraacetic acid (EDTA, pH = 7.5) subsequently. Specimens were embedded in paraffin wax, and sagittal sections of 5 μm thickness were cut for staining.

Laser Confocal Scanning

Mandible was immersed in phosphate-buffered saline containing 4,6-diamidino-2-phenylindole (DAPI, Mengbio, Chongqing, China) and incubated for 24 hours protected from light. The middle segment of MCC was scanned by a confocal laser scanning microscope (Leica, Germany) with a depth of 60 μm and a spacing of 2 μm for imaging.[26] The scanning channel of the DAPI was 405 nm.

Micro-CT Analysis

The subchondral bone structure of TMJ was analyzed by micro-CT (Viva CT 40, Scanco Medical), and scans were performed at 70 kV and 140 mAs at 10.5 μm per layer, and changes in condylar morphology and bone destruction in different areas were visualized on the 3D images. According to the literature,[27] a cubic region of interest (0.3 × 0.3 × 0.3 mm^3) in the cartilage was selected from the junction of cartilage and subchondral bone to observe the longitudinal changes in the subchondral bone of the condyle. The bone volume-to-tissue volume ratio (BV/TV), trabecular thickness (Tb.Th), trabecular separation (Tb.Sp), and trabecular number (Tb.N) were measured for the analysis of bone trabecular microstructure.

Scanning Electron Microscopy

Condyle was dehydrated with gradient ethanol (25–100%) for approximately 1–2 hours per concentration of ethanol and dried in liquid CO_2 for conventional critical point drying. Gold was coated to observe the condylar cartilage surface under the scanning electron microscope (SEM, S-3000N, Japan) at 20 kV with a point resolution of 15 nm and a magnification of 1500 X.

Table 1 Sequences of Primers for the PCR Assays

Primers for Genotyping	Sequences
Common	GCCTGAGAGCTGTAGGCCC
Wild Type	GGAATGGAAAATAGCTCCTGCC
Mutant Reverse	GACAGTATCGGCCTCAGGAA

ROS Staining and Measurement

Fresh discs were cut into 6 μm frozen sections, and the middle segments of discs were selected and assayed for ROS with 2',7'-dichlorofluorescein-diacetate (DCFHDA) according to the manufacturer's instructions. The sections were soaked in 1X washing solution for 10 minutes, covered by probe solution and incubated at 37°C for 30 minutes. Fluorescent microscope was used for image observation and acquisition. The sections from con group that did not receive the overloading force served as the negative control for staining (Figure S1C).

Histological Staining and Scoring

The histological changes of condylar cartilage were observed by staining the condylar sagittal sections using Safranin O and fast green staining solution (SO&FG, Solarbio, China). Paraffin sections were dewaxed to water, stained with freshly prepared Weigert staining solution for 3 minutes, washed and immersed in acidic differentiation solution for 15 seconds, then immersed in fast green staining solution for 4 minutes, subsequently washed with weak acid solution for 15 seconds. Finally, the slices were soaked in Safranin O staining solution for 8 minutes, before routinely dehydrated and sealed. The middle segments of specimens were scored according to the modified Mankin scoring system, including surface fissuring (0,1,2,3), pericellular matrix staining (0,1,2), spatial arrangements of chondrocytes (0,1,2,3), and interterritorial matrix staining (0,1,2,3). Three peers were invited to score the sections with the single blind method, and the final results were averaged as the histological changes in the condyles of each group.

Immunohistochemistry

Paraffin sections were dewaxed to water with xylene and gradient alcohol, completely immersed in antigen retrieval solution (Citrate Antigen Retrieval Solution, Coolaber, China) with an autoclave heated under water for 15 minutes, then cooled naturally to room temperature. According to the manufacturer's instructions (SP-0022, Bioss, China), 3% H_2O_2 deionized water was used to block endogenous peroxidase activity, and 10% normal goat serum was added dropwise for 20 minutes, then slides were incubated with the following primary antibody individually at 4°C overnight: Nrf2 (Bioss, China, 1:200), superoxide dismutase 2 (SOD2, Bioss, China, 1:150), NADPH oxidase 2 (NOX2, Bioss, China, 1:50), matrix metalloproteinase 13 (MMP13, Bioss, 1:100), heme oxygenase 1 (HO-1, Servicebio, China, 1:50), NAD(P)H quinone dehydrogenase 1 (NQO-1, Beyotime, China, 1:50), Kelch like ECH associated protein 1 (Keap1, Servicebio, China, 1:50). The samples were incubated with biotinylated secondary antibody (IgG) and horseradish enzyme-labeled streptavidin working solution (S-A/HRP) for 30 minutes, respectively. Finally, 3.3-diaminobenzidine tetrahydrochloride (DAB) substrate was added dropwise to the slides and observed under the microscope for color reaction of slides, hematoxylin was used to re-stain slides and then placed in flowing water to return to blue, followed by transparency in xylene and gradient alcohol, neutral gum was used to seal the sections. The staining results were scanned and imaged by Olympus scanner (VS-200, Japan) and analyzed. Five sections of 50*50 mm^2 size in each group were randomly selected for semi-quantitative analysis using the Image-Pro Plus 6.0 image analysis system (Media Cybernetics, Rockville, MD), and the results were statistically analyzed by IOD values for mean and variance.

Statistical Analyses

Statistical analysis of the above results was performed with GraphPad Prism 9.0.0 data analysis software. Multiple comparisons were evaluated by one-way analysis of variance (ANOVA), and two groups were compared by multiple *t*-tests. P-value <0.05 was considered statistically significant.

Results

Oxidative Stress Increases in Early MCC Degeneration

ROS staining in the articular discs demonstrated that the ROS content in the articular discs increased with increasing time of force overloading, suggesting an increase in oxidative stress (Figure 1A). The extracellular matrix of MCC increased, the number of superficial fibrous cells decreased, and the number of chondrocytes increased after 5 days of induction. MCC degeneration became obvious, the superficial extracellular matrix decreased, the number of chondrocytes in each

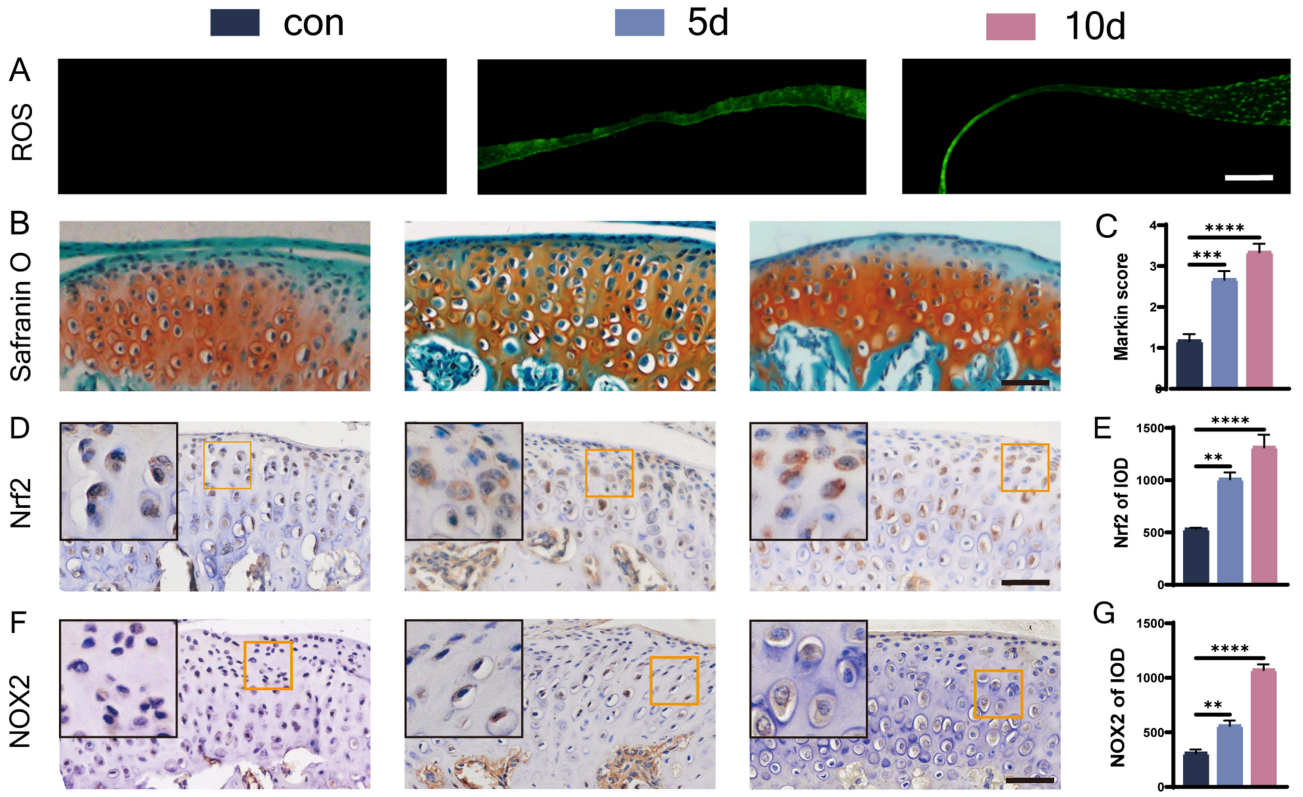

Figure 1 ROS staining and morphological changes of condylar cartilage under overloading force and expression of oxidative stress markers. (**A**) ROS staining, bar=100 μm; (**B** and **C**) S&O staining and Markin score of condylar cartilage, bar=50 μm; (**D**–**G**) immunohistochemical staining and IOD statistics of Nrf2 (**D** and **E**), NOX2 (**F** and **G**), bar=50 μm. The orange boxed area in the image is magnified in the upper left corner. n= 6, **P<0.01, ***P<0.001, and ****P<0.0001 indicate significant differences between groups.

layer decreased, the cell distribution was irregular, and a cell-free zone appeared in the 10 d group (Figure 1B). The Markin score indicated that chondrogenic degeneration was more significant after longer periods of force overloading (Figure 1C). We used immunohistochemical staining to observe changes in the expression of Nrf2 and the oxidative stress marker NOX2 (Figure 1D and F), which is a major source of vascular ROS in condylar chondrocytes. Positive cells were observed at the junction of the proliferative and prehypertrophic layers in the 5 d group. In the 10 d group, more positive cells were concentrated in the prehypertrophic layer. The expression of Nrf2 and NOX2 gradually increased in all layers of the condylar cartilage with a prolonged duration of the overloading force prolonged, as shown by the IOD values (Figure 1E and G).

Nrf2 Knockout Aggravates Early MCC Degeneration

To explore the role of Nrf2 in early MCC degeneration, an overloading force was applied to Nrf2-/- and Nrf2+/+ mice. SEM showed that the MCC surface underwent fibrillation and defect formation after force overloading (Figure 2A). The surface of MCC between groups was rougher in the 10-day groups than in the 5-day groups. Cartilage superficial destruction was more obvious in the MCC of Nrf2-/- mice. The condylar surface of Nrf2-/- mice was even depressed in the N-10E group. Laser confocal microscopy showed that the condylar chondrocytes of Nrf2-/- mice were arranged nonuniformly and that the hypocellular zones were more extensive (Figure 2B). Compared with the N-5E group, the chondrocytes were arranged more irregularly, and chondrocytes were significantly reduced in the N-10E group. Micro CT image analysis showed that there was no significant difference between groups' morphological parameters of condylar subchondral bone as the time of force loading increased (Figure S2A, B). SO&FG staining of the condylar cartilage demonstrated that MCC degeneration under an overloading force was more obvious after Nrf2 knockout, manifested as a reduced extracellular matrix, a decreased number of proliferative and superficial cells, and more

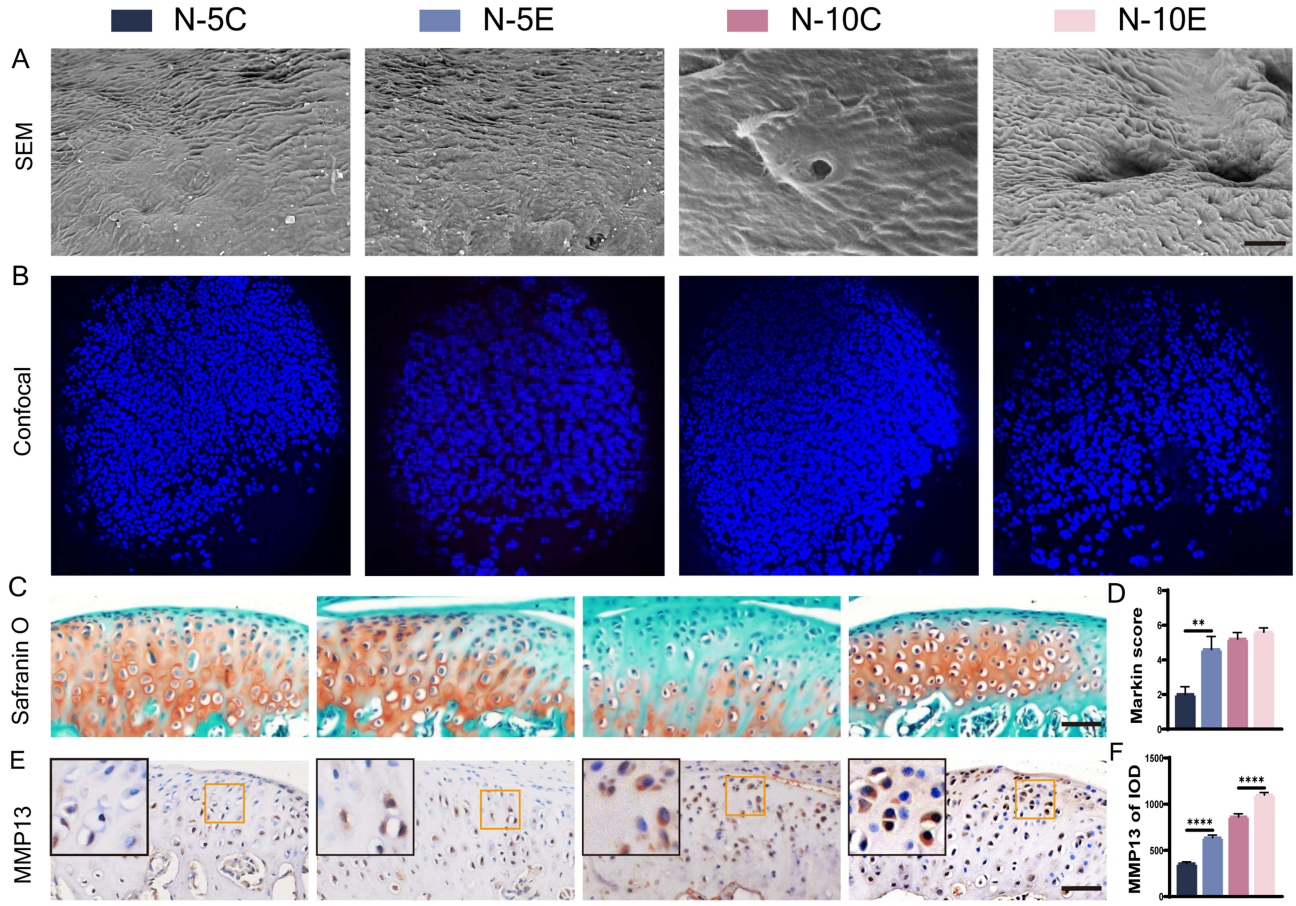

Figure 2 MCC degeneration of Nrf2-/- mouse and Nrf2+/+ mouse condyles under overloading force. (**A**) SEM of condylar cartilage surface, bar=150 μm; (**B**) laser confocal microscopy of Nrf2-/- mouse and Nrf2+/+ mouse condyles; (**C** and **D**) S&O staining and Markin score of condyles under overloading force, bar=50 μm; (**E** and **F**) immunohistochemical staining and IOD value statistics of MMP13, bar=50 μm. The orange boxed area in the images is magnified in the upper left corner. n= 5, **P<0.01, ****P<0.0001 indicate significant differences between groups.

disorganized cell arrangement (Figure 2C and D). Additionally, the increase in MMP13 expression indicated further degradation of the extracellular matrix (Figure 2E and F).

Aggravation of Oxidative Stress in the MCC of Nrf2-/- Mice

ROS staining showed higher fluorescence intensity in the articular discs of Nrf2-/- mice, suggesting that Nrf2 knockout leads to elevated ROS levels (Figure 3A). Between-groups comparison showed that a longer time of force overloading produced a higher ROS level. To further elucidate the role of Nrf2 in oxidative stress, we evaluated the expression of markers associated with oxidative stress in the MCC. Nrf2 staining showed that in the Nrf2-/- groups, positive cells were barely detectable, and Nrf2 expression was elevated in Nrf2+/+ mice under a sustained force (Figure 3B and E). Nrf2 knockout increased NOX2 expression while upregulating SOD2 expression (Figure 3C, D, F and G). The differences were more pronounced between the 10-day groups than between the 5-day groups.

Cardamonin Alleviates Early MCC Degeneration Induced by an Overloading Force

To verify the role of Nrf2 in MCC degeneration, mice were pretreated with an intraperitoneal injection of cardamonin to activate Nrf2. The condylar surface under force induction was observed by SEM (Figure 4A), and condylar cartilage damage became more severe with an increasing overloading force. The MCC surface that did not receive cardamonin showed obvious fibrillation and defect formation, while the MCC surface damage that received cardamonin was mitigated to some extent. Confocal microscopy showed that the condylar cartilage cells were more uniformly distributed,

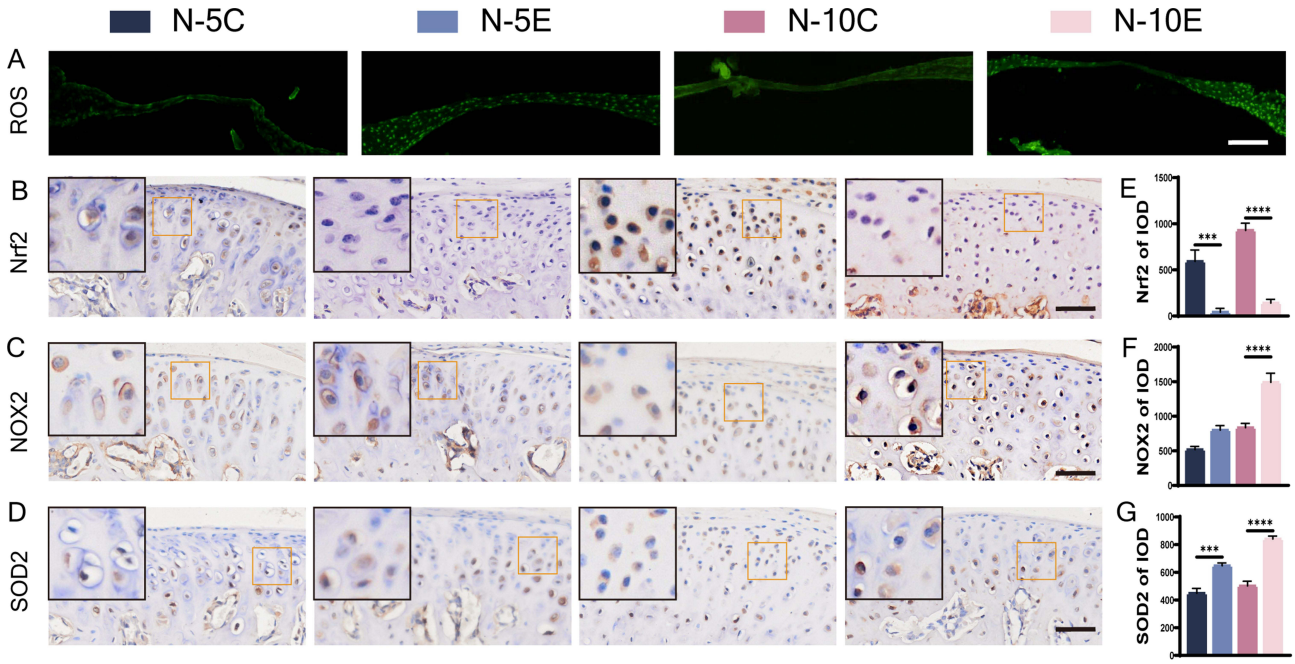

Figure 3 ROS staining and immunohistochemical staining of oxidative stress markers in condylar cartilage of Nrf2-/- mice and Nrf2+/+ mice. (**A**) ROS staining, bar=100 μm; (**B**–**D**) immunohistochemical staining of Nrf2 (**B**), NOX2 (**C**), SOD2 (**D**) and their IOD value statistics (**E**–**G**), bar=50 μm. The orange boxed area in the image is magnified in the upper left corner. n= 5, ***P<0.001, ****P<0.0001 indicate significant differences between groups.

more closely packed, and more numerous in the C-5E and C-10E groups (Figure 4B). Morphological parameters of subchondral bone were analyzed, and the results did not reveal statistically significant differences under an overloading force with and without cardamonin treatment (Figure S3A, B). Compared with the control groups, SO&FG staining revealed that the number of cells in the superficial layer of the MCC and retention of the extracellular matrix were more preserved after cardamonin treatment (Figure 4C and D). MMP13 staining indicated that treatment with cardamonin attenuated degradation of the extracellular matrix (Figure 4E and F).

Cardamonin Alleviates Oxidative Stress via Nrf2 Pathway Activation

The ROS content in the discs of mice treated with and without cardamonin was measured separately (Figure 5A). The ROS content was lower in the discs of mice pretreated with cardamonin, suggesting that the oxidative stress reaction was alleviated. The changes in oxidative stress markers within MCC were observed further. Nrf2 expression was significantly increased (Figure 5B and H), NOX2 expression was decreased (Figure 5C and I), and oxidase SOD2 expression was downregulated after cardamonin treatment (Figure 5D and J); their changing trends were more pronounced in the 10-day groups than in the 5-day groups. Additionally, the expression of downstream targets related to the Nrf2 pathways, such as NQO-1 and HO-1, was also elevated. The expression of Keap1, a downstream target antagonistic to Nrf2, was reduced, and statistical analysis revealed that the change between groups was more significant in the 5-day groups than in the 10-day groups (Figure 5E–G, K–M).

Discussion

TMJ diseases are characterized by cartilage degeneration, and their occurrence is closely related to imbalanced oxidative stress.[28] Currently, studies have been conducted on articular cartilage-induced lesions using inflammatory factors or surgery. In these models, arthropathy progresses to osteoarthritis, the late stage of cartilage degeneration, for which specific changes and underlying mechanisms cannot be observed at the early stage of degeneration.[29,30] Intervention at the early stage of MCC degeneration may prevent joint diseases from progressing to more severe inflammation and disability, which can cause irreversible damage. Fang's study demonstrated that overloading force-induced MCC

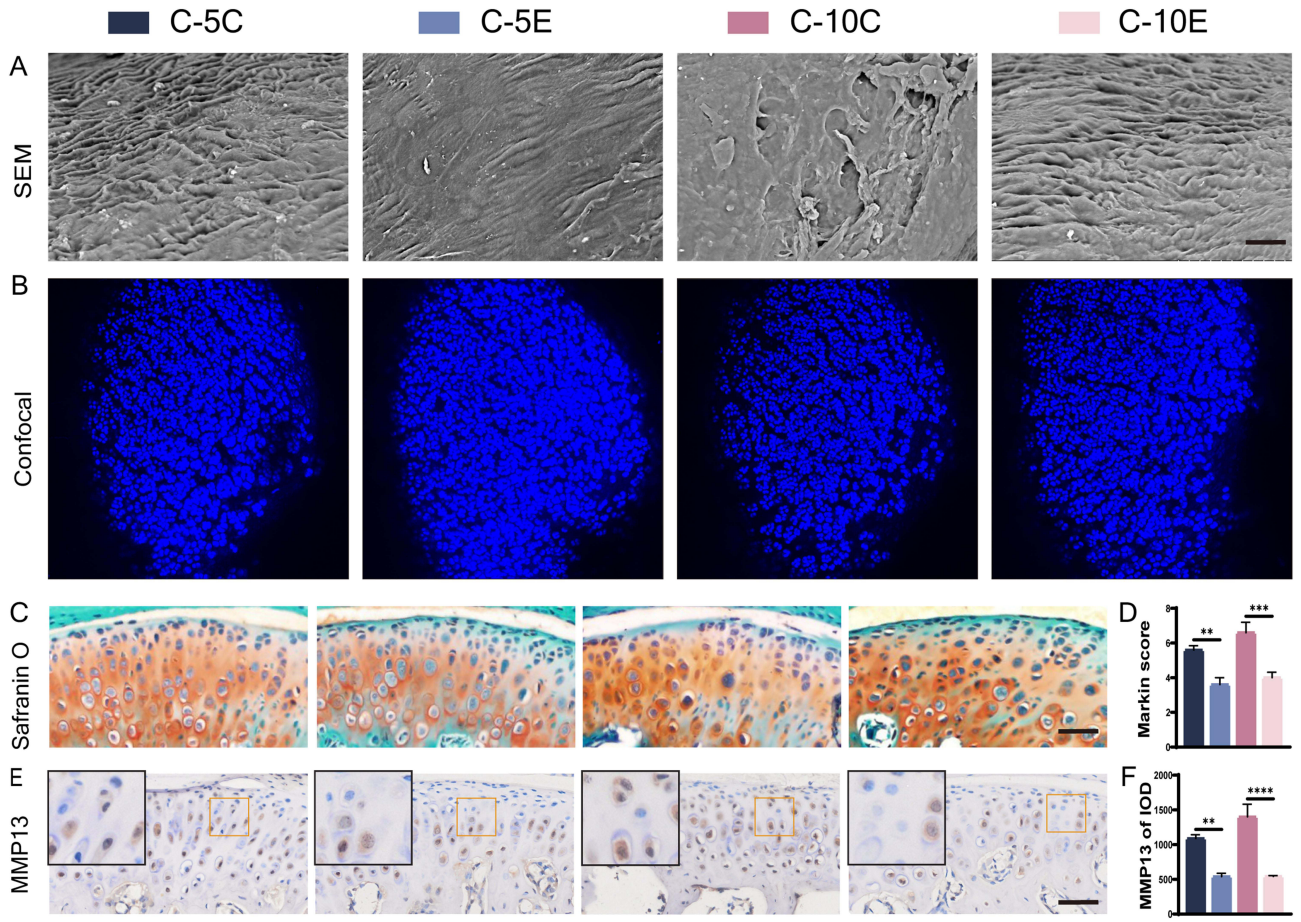

Figure 4 MCC degeneration under overloading force after cardamonin or blank drugs treatment, bar=150 μm. (**A**) SEM of condylar cartilage surface; (**B**) laser confocal microscopy of mouse condyles; (**C** and **D**) S&O staining and Markin score of condyles under overloading force, bar=50 μm; (**E** and **F**) immunohistochemical staining and IOD value statistics for MMP13, bar=50 μm. The orange boxed area in the images is magnified in the upper left corner. n= 6, **P<0.01, ***P<0.001, ****P<0.0001 indicate significant differences between groups.

degeneration is a sequential process, a finding that was consistent with the natural development of the disease process.[14] Therefore, we induced early MCC degeneration using an overloading force.

We observed that the MCC degeneration and the expression of Nrf2 and NOX2 were more obvious in 10-day group of force overloading than in 5-day groups, whereas changes in Nrf2 downstream factors were more pronounced between the 5-day groups. Therefore, we conclude that with the extension of the force loading, the aggravation of MCC degeneration was accompanied by the increase of oxidative stress, and the downstream factors may be more sensitive to the overloading force at the beginning of the degeneration. Two previous studies have found that Nrf2 expression increases in chondrocytes treated with IL-1β in vitro,[23,24] while curcumin, a natural extract that also has anti-inflammatory and antioxidant properties, decreases Nrf2 expression and alleviates cartilage destruction in late degeneration stage.[23] Therefore, it seems that Nrf2 could be used as a therapeutic target in the early stage of cartilage degeneration, which is supposed to mitigate the degeneration process to some extent. Overloading force-induced TMJ degeneration with more distinct stages and specific Nrf2 regulation networks would give more persuasive evidence for mechanism exploration, thus making Nrf2 a mature therapeutic target in MCC degeneration.

Intracellular mitochondria, as the main carriers of oxidative pathways, are the primary source of superoxide, the predecessor of ROS.[31] Once the ROS concentration exceeds the natural scavenging capacity of the antioxidant defense system, oxidative stress occurs.[31] Therefore, ROS are frequently mentioned in relevant studies as one of the most reliable markers of oxidative stress, and their measurement is mainly performed by DHE probe staining. In both in vitro and in vivo experiments, the measurements are usually obtained by direct staining of cells and corresponding fresh animal

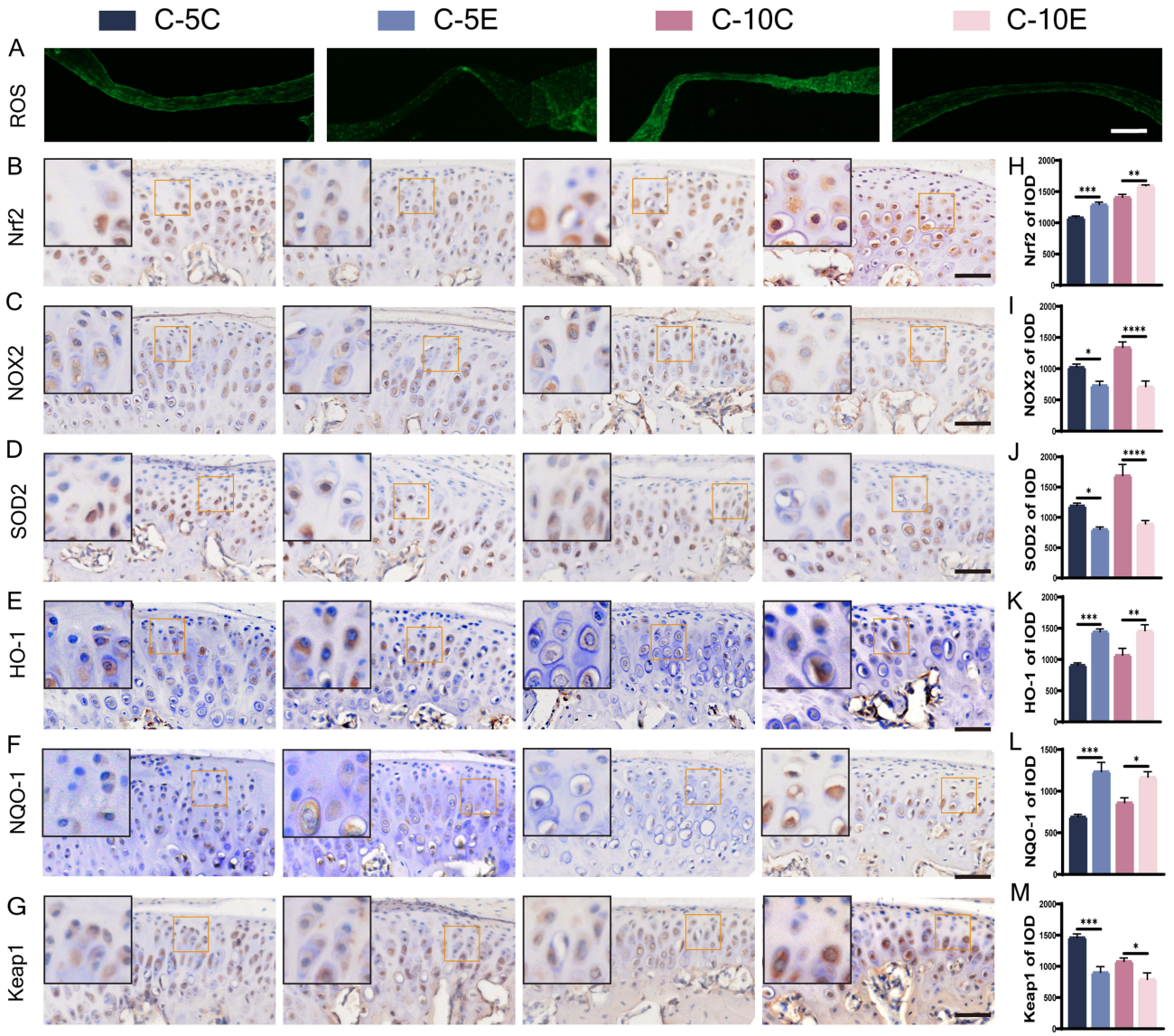

Figure 5 ROS staining and immunohistochemical staining for markers of oxidative stress in condylar cartilage of mice accepting cardamonin-treated and blank drug groups. (**A**) ROS staining, bar=100 μm; (**B–M**) immunohistochemical staining for Nrf2 (**B**), NOX2 (**C**), SOD2 (**D**), HO-1 (**E**), NQO-1 (**F**), Keap1 (**G**) and their IOD value statistics (**H–M**), bar=50 μm. The orange boxed area in the image is magnified in the upper left corner. n = 6, *P<0.05, **P<0.01, ***P<0.001, ****P<0.0001 indicate significant differences between groups.

tissues.[25,32,33] Determination of the ROS content may be challenging for joint-related experiments because of the small amount of tissue available in mouse joints and the nontransparency of cartilage. Phenotypic identification of oxidative stress after ROS overproduction is generally obtained by staining articular cartilage after decalcification,[23,34] and little direct ROS staining is observed in fresh cartilage. We stripped fresh TMJ discs for direct DHE staining on frozen slides to observe ROS production. The findings were consistent with the changes in oxidative stress markers observed within the MCC. Of course, if there were a way to detect ROS levels in cartilage in the future, the results would be even more convincing.

Our results showed that Nrf2 exhibited anti-oxidative effect in the early MCC degeneration by down-regulated ROS. As the sensible maker of ROS, we observed that the expression of SOD2 was synchronous with ROS production. The similar expression relevance between ROS and SOD2 could be found in other studies.[35,36] SOD2 and Nrf2 are both important anti-oxidative factors, and they were found to perform similar expression trend in some studies related to oxidative stress.[37,38] However, our results showed that SOD2 increased when Nrf2 was knocked out and decreased

following Nrf2 activation. It seems that SOD2 played compensatory role of Nrf2 in anti-oxidative process in early MCC degeneration. Zhu's study reported that the expression of Nrf2 and SOD2 was not always positively correlated and also suggested that Nrf2 plays a different role in regulating the expression of SOD in different cell types.[39] This seems to explain our results, perhaps there are other mechanisms between Nrf2 and SOD2 in condylar chondrocytes, and further exploration is needed to understand the internal mechanism of SOD2 regulating MCC degeneration.

Conclusion

Our study demonstrated that Nrf2, a crucial antioxidant factor, can serve as a potential target to alleviate early MCC degeneration induced by mechanical overloading forces. Cardamonin, as an Nrf2 activator, may protect the overloading force-induced condylar cartilage by regulating oxidative stress. This study may help clarify the mechanism of early MCC degeneration and alleviate early TMJ diseases.

Abbreviations

TMJ, temporomandibular joint; Nrf2, erythroid 2-related factor 2; MCC, mandibular condylar cartilage; NOX2, NADPH oxidase 2; SOD2, superoxide dismutase 2; ROS, reactive oxygen species; ESR, electron spin resonance; DCFHDA, 2',7'-dichlorofluorescein-diacetate; PCR, polymerase chain reaction; SEM, scanning electron microscopy; DAPI, 4,6-diamidino-2-phenylindole; MMP13, matrix metalloproteinase 13; HO-1, heme oxygenase 1; NQO-1, NAD(P)H quinone dehydrogenase 1; Keap1, Kelch like ECH associated protein 1.

Ethical Statement

This study was approved by the Animal Ethics Committee of Chongqing Medical University (AECCMU-2020-004), and all experiments followed the National Institutes of Health's Guidelines for the Care and Use of Laboratory Animals.

Author Contributions

All authors made a significant contribution to the work reported, whether that is in the conception, study design, execution, acquisition of data, analysis and interpretation, or in all these areas; took part in drafting, revising or critically reviewing the article; gave final approval of the version to be published; have agreed on the journal to which the article has been submitted; and agree to be accountable for all aspects of the work.

Funding

This work was supported by China Postdoctoral Science Foundation (2018M640902 to Y.H.).

Disclosure

All authors declare no conflicts of interest in this work.

References

1. Valesan LF, Da-Cas CD, Réus JC, et al. Prevalence of temporomandibular joint disorders: a systematic review and meta-analysis. *Clin Oral Invest*. 2021;25(2):441–453. doi:10.1007/s00784-020-03710-w
2. Tanaka E, Detamore MS, Mercuri LG. Degenerative disorders of the temporomandibular joint: etiology, diagnosis, and treatment. *J Dent Res*. 2008;87(4):296–307. doi:10.1177/154405910808700406
3. Kmeid E, Nacouzi M, Hallit S, Rohayem Z. Prevalence of temporomandibular joint disorder in the Lebanese population, and its association with depression, anxiety, and stress. *Head Face Med*. 2020;16(1):19. doi:10.1186/s13005-020-00234-2
4. Santana-Mora U, López-Cedrún J, Suárez-Quintanilla J, et al. Asymmetry of dental or joint anatomy or impaired chewing function contribute to chronic temporomandibular joint disorders. *Ann Anat*. 2021;238:151793. doi:10.1016/j.aanat.2021.151793
5. Helmick CG, Felson DT, Lawrence RC, et al. Estimates of the prevalence of arthritis and other rheumatic conditions in the United States: part I. *Arth Rheum*. 2008;58(1):15–25. doi:10.1002/art.23177
6. Gualtierotti R, Marzano A, Spadari F, Cugno M. Main oral manifestations in immune-mediated and inflammatory rheumatic diseases. *JCM*. 2018;8(1):21. doi:10.3390/jcm8010021
7. Minervini G, Franco R, Marrapodi MM, et al. Correlation between Temporomandibular Disorders (TMD) and posture evaluated trough the Diagnostic Criteria for Temporomandibular Disorders (DC/TMD): a systematic review with meta-analysis. *JCM*. 2023;12(7):2652. doi:10.3390/jcm12072652

8. Minervini G, Franco R, Marrapodi MM, Ronsivalle V, Shapira I, Cicciù M. Prevalence of temporomandibular disorders in subjects affected by Parkinson disease: a systematic review and metanalysis. *J Oral Rehabil*. 2023;50(9):877–885. doi:10.1111/joor.13496
9. Stegenga B. Nomenclature and classification of temporomandibular joint disorders. *J Oral Rehabil*. 2010;37(10):760–765. doi:10.1111/j.1365-2842.2010.02146.x
10. Wang XD, Zhang JN, Gan YH, Zhou YH. Current understanding of pathogenesis and treatment of TMJ osteoarthritis. *J Dent Res*. 2015;94(5):666–673. doi:10.1177/0022034515574770
11. Li W, Hu S, Chen X, Shi J. The antioxidant resveratrol protects against chondrocyte apoptosis by regulating the COX-2/NF-κB pathway in created temporomandibular osteoarthritis. *Biomed Res Int*. 2021;2021:1–7. doi:10.1155/2021/9978651
12. Li H, Zhang XY, Wu TJ, et al. Endoplasmic reticulum stress regulates rat mandibular cartilage thinning under compressive mechanical stress. *J Biol Chem*. 2013;288(25):18172–18183. doi:10.1074/jbc.M112.407296
13. Zhang Y, Liu Q, Xu X, et al. Long-term effect of bilateral anterior elevation of occlusion on the temporomandibular joints. *Oral Dis*. 2021:13914. doi:10.1111/odi.13914
14. Fang L, Ye Y, Tan X, Huang L, He Y. Overloading stress–induced progressive degeneration and self-repair in condylar cartilage. *Ann NY Acad Sci*. 2021;1503(1):72–87. doi:10.1111/nyas.14606
15. Merry P, Winyard PG, Morris CJ, Grootveld M, Blake DR. Oxygen free radicals, inflammation, and synovitis: and synovitis: the current status. *Ann Rheum Dis*. 1989;48(10):864–870. doi:10.1136/ard.48.10.864
16. Halliwell B, Gutteridge JMC. Free radicals in biology and medicine. *J Free Rad Biol Med*. 1985;1(4):331–332. doi:10.1016/0748-5514(85)90140-0
17. Kawai Y, Kubota E, Okabe E. Reactive oxygen species participation in experimentally induced arthritis of the temporomandibular joint in rats. *J Dent Res*. 2000;79(7):1489–1495. doi:10.1177/00220345000790071001
18. Milam SB, Zardeneta G, Schmitz JP. Oxidative stress and degenerative temporomandibular joint disease: a proposed hypothesis. *J Oral Maxillofac Surg*. 1998;56(2):214–223. doi:10.1016/S0278-2391(98)90872-2
19. Basi DL, Velly AM, Schiffman EL, et al. Human temporomandibular joint and myofascial pain biochemical profiles: a case-control study. *J Oral Rehabil*. 2012;39(5):326–337. doi:10.1111/j.1365-2842.2011.02271.x
20. Yamaza T, Masuda KF, Atsuta I, Nishijima K, Kido MA, Tanaka T. Oxidative stress-induced DNA damage in the synovial cells of the temporomandibular joint in the rat. *J Dent Res*. 2004;83(8):619–624. doi:10.1177/154405910408300807
21. Lepetsos P, Papavassiliou AG. ROS/oxidative stress signaling in osteoarthritis. *Biochim Biophys Acta Mol Basis Dis*. 2016;1862(4):576–591. doi:10.1016/j.bbadis.2016.01.003
22. Omidpanah N, Ebrahimi S, Vaisi Raygani A, Mozafari H, Rezaei M. Total Antioxidant capacity, catalase activity and salivary oxidative parameters in patients with temporomandibular disorders. *Front Dent*. 2020. doi:10.18502/fid.v17i16.4179
23. Jiang C, Luo P, Li X, Liu P, Li Y, Xu J. Nrf2/ARE is a key pathway for curcumin-mediated protection of TMJ chondrocytes from oxidative stress and inflammation. *Cell Stress Chaperones*. 2020;25(3):395–406. doi:10.1007/s12192-020-01079-z
24. Peng YJ, Lu JW, Lee CH, et al. Cardamonin attenuates inflammation and oxidative stress in interleukin-1β-stimulated osteoarthritis chondrocyte through the Nrf2 Pathway. *Antioxidants*. 2021;10(6):862. doi:10.3390/antiox10060862
25. Qi W, Boliang W, Xiaoxi T, Guoqiang F, Jianbo X, Gang W. Cardamonin protects against doxorubicin-induced cardiotoxicity in mice by restraining oxidative stress and inflammation associated with Nrf2 signaling. *Biomed Pharmacother*. 2020;122:109547. doi:10.1016/j.biopha.2019.109547
26. He Y, Zhang M, Huang AY, Cui Y, Bai D, Warman ML. Confocal imaging of mouse mandibular condyle cartilage. *Sci Rep*. 2017;7(1):43848. doi:10.1038/srep43848
27. Zhang J, Jiao K, Zhang M, et al. Occlusal effects on longitudinal bone alterations of the temporomandibular joint. *J Dent Res*. 2013;92(3):253–259. doi:10.1177/0022034512473482
28. Rodríguez de Sotillo D, Velly AM, Hadley M, Fricton JR. Evidence of oxidative stress in temporomandibular disorders: a pilot study. *J Oral Rehabil*. 2011;38(10):722–728. doi:10.1111/j.1365-2842.2011.02216.x
29. Kruisbergen NNL, Di Ceglie I, van Gemert Y, et al. Nox2 deficiency reduces cartilage damage and ectopic bone formation in an experimental model for osteoarthritis. *Antioxidants*. 2021;10(11):1660. doi:10.3390/antiox10111660
30. Ni S, Li D, Wei H, Miao KS, Zhuang C. PPARγ attenuates interleukin-1β-induced cell apoptosis by inhibiting NOX2/ROS/p38MAPK activation in osteoarthritis chondrocytes. *Oxid Med Cell Longev*. 2021;2021:1–15. doi:10.1155/2021/5551338
31. Gandhi S, Abramov AY. Mechanism of oxidative stress in neurodegeneration. *Oxid Med Cell Longev*. 2012;2012:1–11. doi:10.1155/2012/428010
32. Jin J, Qiu S, Wang P, et al. Cardamonin inhibits breast cancer growth by repressing HIF-1α-dependent metabolic reprogramming. *J Exp Clin Cancer Res*. 2019;38(1):377. doi:10.1186/s13046-019-1351-4
33. Chen Z, Zhong H, Wei J, et al. Inhibition of Nrf2/HO-1 signaling leads to increased activation of the NLRP3 inflammasome in osteoarthritis. *Arthritis Res Ther*. 2019;21(1):300. doi:10.1186/s13075-019-2085-6
34. Stojić V, Glišić B, Djukić L, et al. Mandibular lateral deviation induces alteration in vascular endothelial growth factor expression and oxidative stress/nitric oxide generation in rat condyle, synovial membrane and masseter muscle. *Arch Oral Biol*. 2020;110:104599. doi:10.1016/j.archoralbio.2019.104599
35. Ji G, Lv K, Chen H, et al. MiR-146a regulates SOD2 expression in H2O2 stimulated PC12 cells. *PLoS One*. 2013;8(7):e69351. doi:10.1371/journal.pone.0069351
36. Smith GR, Shanley DP. Computational modelling of the regulation of Insulin signalling by oxidative stress. *BMC Syst Biol*. 2013;7(1):41. doi:10.1186/1752-0509-7-41
37. Dong J, Zhang L, Ruan B, et al. NRF2 is a critical regulator and therapeutic target of metal implant particle-incurred bone damage. *Biomaterials*. 2022:121742. doi:10.1016/j.biomaterials.2022.121742
38. Ding X, Jian T, Li J, et al. Chicoric acid ameliorates nonalcoholic fatty liver disease via the AMPK/Nrf2/NFκB signaling pathway and restores gut microbiota in high-fat-diet-fed mice. *Oxid Med Cell Longev*. 2020;2020:1–20. doi:10.1155/2020/9734560
39. Zhu H, Jia Z, Misra BR, et al. Nuclear factor E2-related factor 2-dependent myocardiac cytoprotection against oxidative and electrophilic stress. *Cardiovasc Toxicol*. 2008;8(2):71–85. doi:10.1007/s12012-008-9016-0